

Taming Self-Supervised Learning for Presentation Attack Detection: In-Image De-Folding and Out-of-Image De-Mixing

Haozhe Liu^{†,1,2,3,4}, Zhe Kong^{†,1,2,3}, Raghavendra Ramachandra^{†,4}, Feng Liu^{*1,2,3}, Linlin Shen^{1,2,3},
Christoph Busch⁴

¹Computer Vision Institute, College of Computer Science and Software Engineering,

²SZU Branch, Shenzhen Institute of Artificial Intelligence and Robotics for Society,

³Guangdong Key Laboratory of Intelligent Information Processing, Shenzhen University, Shenzhen 518060, China

⁴Norwegian Biometrics Laboratory (NBL), Norwegian University of Science and Technology (NTNU), Gjøvik 2818, Norway
{liuhaozhe2019, kongzhe2020}@email.szu.edu.cn; {raghavendra.ramachandra, christoph.busch}@ntnu.no; {feng.liu, llshen}@szu.edu.cn

Abstract

Biometric systems are vulnerable to the Presentation Attacks (PA) performed using various Presentation Attack Instruments (PAIs). Even though there are numerous Presentation Attack Detection (PAD) techniques based on both deep learning and hand-crafted features, the generalization of PAD for unknown PAI is still a challenging problem. The common problem with existing deep learning-based PAD techniques is that they may struggle with local optima, resulting in weak generalization against different PAs. In this work, we propose to use self-supervised learning to find a reasonable initialization against local trap, so as to improve the generalization ability in detecting PAs on the biometric system. The proposed method, denoted as IF-OM, is based on a global-local view coupled with De-Folding and De-Mixing to derive the task-specific representation for PAD. During De-Folding, the proposed technique will learn region-specific features to represent samples in a local pattern by explicitly maximizing cycle consistency. While, De-Mixing drives detectors to obtain the instance-specific features with global information for more comprehensive representation by maximizing topological consistency. Extensive experimental results show that the proposed method can achieve significant improvements in terms of both face and fingerprint PAD in more complicated and hybrid datasets, when compared with the state-of-the-art methods. Specifically, when training in CASIA-FASD and Idiap Replay-Attack, the proposed method can achieve 18.60% Equal Error Rate (EER) in OULU-NPU and MSU-MFSD, exceeding baseline performance by 9.54%. *Code will be made publicly available.*

Introduction

With the applications in mobile phone unlocking, access control, payment tool and other security scenarios, biometric systems are widely used in our daily lives. Among the most popular biometric modalities, fingerprint and face play vital roles in numerous access control applications. However, several reported studies (Ramachandra and Busch 2017; Singh et al. 2020) have demonstrated that the existing systems are easily spoofed by presentation attacks (PAs) made from

some low-cost materials, e.g. Rigid Mask for face (Heusch et al. 2020) and silica-gel for fingerprint (Liu et al. 2021b). These issues raise wide concerns about the vulnerability of biometric systems incorporated in access control applications. Therefore it is essential to detect the presentation attacks to achieve reliable biometric applications.

To reliably address the vulnerability of the biometric systems to PAIs, several Presentation Attack Detection (PAD) methods have been proposed (Ramachandra and Busch 2017), which can be divided into hardware and software based methods. Hardware based solutions (Liu et al. 2021a; Heusch et al. 2020; Raghavendra, Raja, and Busch 2015) employ the special types of sensors to capture liveness characteristics. For instance, Heusch et al. (Heusch et al. 2020) adopt short wave infrared (SWIR) imaging technology to detect face PAs, which shows superior performance over similar models working on color images. Light field camera (LFC) is introduced by Raghavendra et al. (Raghavendra, Raja, and Busch 2015) to detect PAs by exploring the variation of the focus between multiple depth images. For fingerprint, an optical coherence tomography (OCT)-based PAD system is designed by Liu et al. (Liu et al. 2021a) to obtain the depth information of fingerprints. Generally speaking, hardware-based solutions are sensor-specific, resulting in strong security but weak applicability because of usability or cost limitations.

Fig. 1 illustrates the recent progress on the software based PAD algorithms that can be categorized into three groups: 1) Input Preprocessing, 2) Model Design and 3) Loss Function. In the case of Input Preprocessing (Liu, Jourabloo, and Liu 2018; Larbi et al. 2018; Chugh and Jain 2021; Wang et al. 2021; Guo et al. 2019), Larbi et al. (Larbi et al. 2018) propose a model, namely DeepColorFASD, which adopts various color spaces (RGB, HSV, YCbCr) as input to achieve the reliable performance of PAD. Despite the improvement, the additional color spaces need to be processed, which will lead to extra computation. Meanwhile, the contribution of different color spaces is limited to improve the generalization against unexpected PAIs. For fingerprint anti-spoofing, a Generative Adversarial Network (GAN) based data augmentation, called Universal Material Generator (UMG), is proposed by Chugh et al. (Chugh and Jain 2021). UMG transfers the style (texture) characteristics between finger-

[†] Equal Contribution

^{*} Corresponding Author: feng.liu@szu.edu.cn

This work was done when Haozhe Liu was a visiting student at NTNU, Gjøvik, Norway

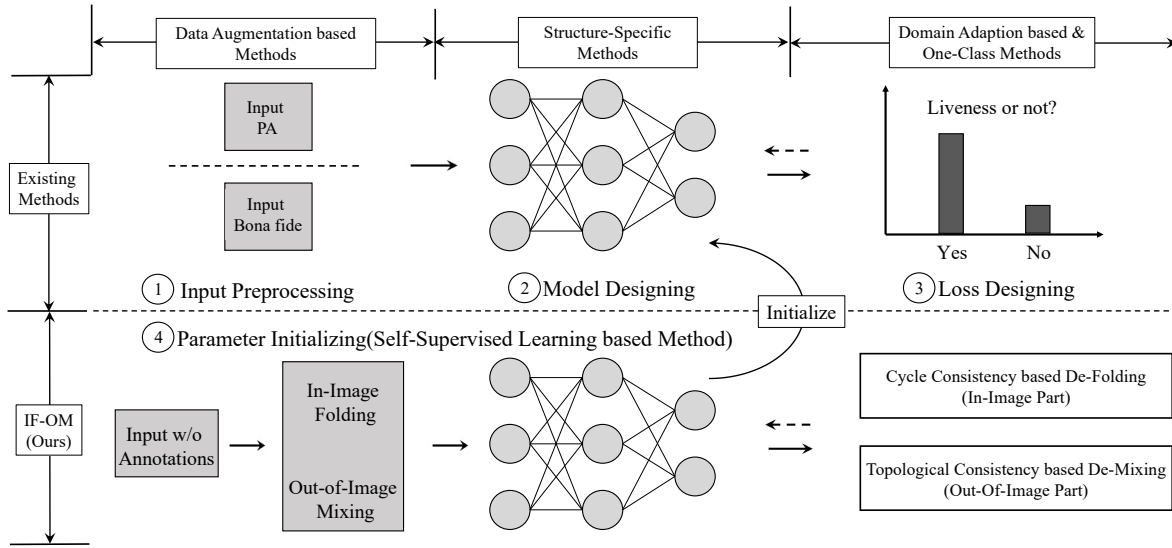


Figure 1: The groups of software based presentation attack detection. Group 1 is Input Preprocessing, Group 2 refers to Model Designing and Group 3 is Loss Function Designing. Different from existing groups, the proposed method investigates the initialization of the PA detector, which can be concluded as an independent solution, i.e. Group 4: Parameter Initializing.

print images to train a robust PA detector. However, such method needs the images from the target material or target capture device to obtain the style characteristics, which might be inaccessible.

Different from Input Preprocessing, the Model Designing approaches pay more attention to the specific CNN based architectures. Many prior works adopt hand-crafted features such as LBP (de Freitas Pereira et al. 2013), HoG (Yang et al. 2013), SIFT (Patel, Han, and Jain 2016) and Surf (Boulkenafet, Komulainen, and Hadid 2016), then employ traditional classifier such as LDA and SVM. But hand-crafted features are sensitive to the noise, illumination and have poor generalization performance. Consequently, structure-specific methods based on convolution neural network (CNN) are proposed. In particular, Liu et al. (Liu, Jourabloo, and Liu 2018) propose a CNN-RNN model to learn auxiliary features, including depth and rPPG, for PAD. A Deep Tree Network (DTN) is proposed by Liu et al. (Liu et al. 2019) to partition the spoof samples into semantic subgroups and detect PAs by routing test samples into the similar clusters. Yu et al. (Yu et al. 2020) propose a Central Difference Convolution (CDC) layer to capture intrinsic detailed patterns via aggregating both intensity and gradient information. By adopting Neural Architecture Search (NAS), the CDC based network can achieve superior performance. Although competitive results can be achieved through specially designed architecture, the cross domain performance of CNN based methods is still limited, leading to the limited application in real scenarios.

To tackle the cross-domain issue, existing works are trying to improve the generalization by training models with specific learning objectives. For example, the one-class loss proposed by George et al. (George and Marcel 2020) tries to learn a compact embedding space for the bona fide class

which is only a special case of attacks. Furthermore, the one-class loss only considers the domain-invariant features and ignores the differences among domains. Hence, Jia et al. (Jia et al. 2020) propose an Asymmetric Triplet Loss to mine the PAD features and design a Single-Side Adversarial Loss to align the mined features between the different domains. However, considering that the CNN based PA detectors are trained in a sophisticated way, the learning objectives might not be successfully trained.

An important interference factor is the initialization of the PA detector. As a general rule, training from scratch and pre-training using ImageNet (Russakovsky et al. 2015) are two common methods. However, in PAD, it is challenging to collect large-scale data, hence, without any prior knowledge, it is difficult to train the model from scratch (i.e. random initialization) to learn discriminative features. On the other side, taking pre-trained model from ImageNet as initialization is also not a proper choice. As a large-scale dataset, the cost of time and computation carried on ImageNet is an over-heavy workload to train new proposed PAD CNN architectures. Meanwhile, face and fingerprint images are quite different from natural images in both texture and context, the pre-trained model is thus not an ideal and reasonable starting point for PAD task.

As shown in Fig.1, in order to solve the addressed problems, a self-supervised learning based method, denoted as IF-OM, is proposed in this paper. Without any annotations, two pretext tasks are designed to train the network, which is finally set as the initialization of the PA detector. Based on the chirality and symmetry of the face and fingerprint, a Cycle Consistency based De-Folding task is designed to force CNN based model to reconstruct the folded images by learning the specific patterns among various regions in faces or fingerprints. To further strengthen the representation, a

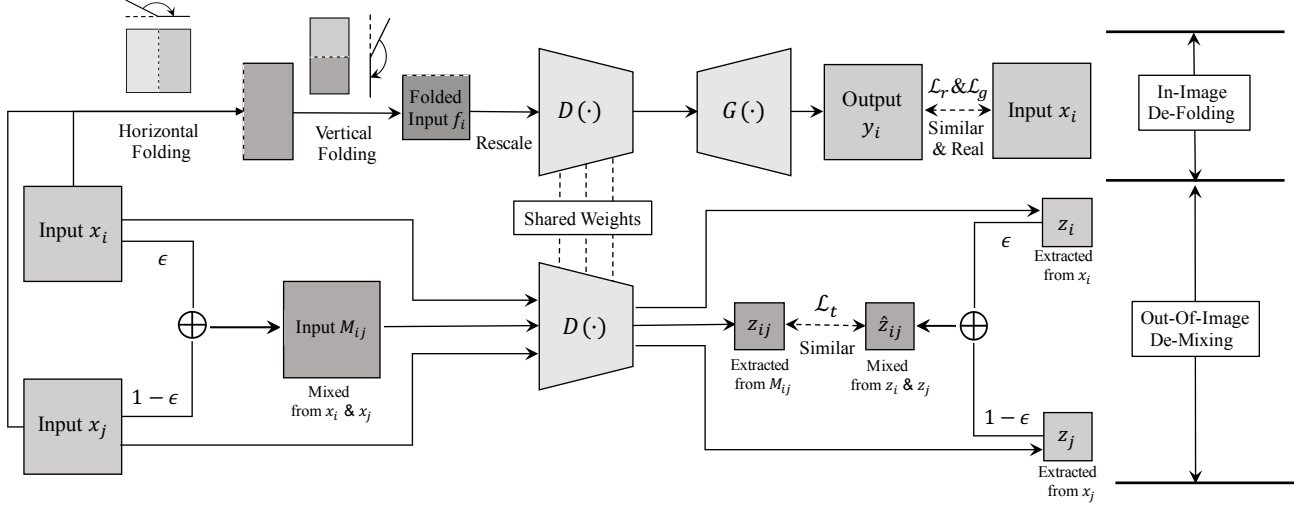


Figure 2: The pipeline of the proposed self-supervised learning based method (IF-OM). The feature extractor $D(\cdot)$ is trained by De-Folding and De-Mixing tasks simultaneously. In De-Folding task, the input image is folded and the target of the model is to reconstruct the image by maximizing the cycle consistency. In De-Mixing task, two images are mixed by a random weight ϵ , and the learning objective is to guarantee the topological/operational consistency between the input space and feature space embedded by $D(\cdot)$. Note that both x_i and x_j are employed for De-Folding, but only the pipeline of x_i is shown in the figure, due to the same processing for x_i and x_j .

Topological Consistency based De-Mixing task is then proposed to facilitate the extraction of global features by disentangling the mixed images from two samples. Without any extra training samples and annotations, the proposed methods can obtain an ideal initialization, which can improve fingerprint PAD baseline from 73.92% to 90.96 % in TDR (True Detection Rate)@1% FDR (False Detection Rate) and promote the EER (Equal Error Rate) of face PAD baseline by 8.12 %. In summary,

- A Cycle Consistency based De-Folding task is designed for fingerprint and face PAD to explore the specific patterns among different regions.
- As a complementary task, Topological Consistency based De-Mixing task is proposed to learn more hierarchical features to better represent images.
- The proposed method, which only works in a lite and unsupervised mode, achieves impressive performance in terms of face and fingerprint PAD.

Related Works

Since this paper mainly focuses on a PAD solution based on self-supervised learning, we review the most representative works of such technology as below. Self-supervised learning refers to learning methods in which CNNs are trained with automatically generated labels and then transferred to other computer vision tasks (Jing and Tian 2020). Based on the categories of the generated labels, self-supervised learning can be roughly divided into generative and contrastive learning. However, both kinds of methods can not be directly used in PAD. As fingerprint and face images for recognition are lack of colorful information, and generally with

low resolution, generative learning, such as image colorization (Zhang, Isola, and Efros 2016) and image super resolution (Ledig et al. 2017), can not be conducted in this case. Meanwhile, for image in-painting (Pathak et al. 2016) and GANs (Goodfellow et al. 2014; Zhu et al. 2017), large-scale data is required to establish a compact feature space, while the dataset for PAD can not meet the requirement. On the other side, face images have strong spatial specification after alignment, while, the spatial relation of fingerprints is weak. Hence, contrastive learning, like predicting the relative position (Doersch, Gupta, and Efros 2015) and rotation (Gidaris, Singh, and Komodakis 2018), is easy for face but too hard for fingerprint. Another group of contrastive learning is instance discrimination, like MoCo (He et al. 2020; Chen et al. 2020b), SimCLR (Chen et al. 2020a) and BYOL (Grill et al. 2020). Through embedding each instance/image into different classes, the mentioned studies have shown solid improvement in natural images. However, in the PAD task, bijective relation between each image and prediction leads model to learn identification rather than PAD features, resulting in poor generalization performance (Wang et al. 2020).

In this paper, a novel self-supervised learning, namely IF-OM, is proposed to improve the performance of PAD. Unlike existing methods, the proposed method is free of any annotations and extra data, and pays more attention to the specification of the face and fingerprint. Particularly, two pretext tasks, De-Mixing and De-Folding, are proposed to search a reasonable initialization for the PA detector. As an in-image part, De-Folding explores the properties of face and fingerprint, such as chirality and symmetry. While, in the out-of-image part, De-Mixing requires the model to embed images

into a distinguishable feature space with the same topological structure in the input space. By drawing De-Folding and De-Mixing simultaneously, adequate PAD features are extracted, which can be useful to detect PAs. Extensive experiments clearly show the significant improvements in performance of face and fingerprint PAD.

Proposed Method

Figure 2 presents the block diagram of the proposed IF-OM, which adopts De-Folding and De-Mixing to reliably capture the hierarchical features useful for PAD. The goal of De-Folding is to reconstruct the raw image from the folded image. Since the folded image and the corresponding ground truth can be easily obtained, the model in this task is directly trained by maximizing Cycle Consistency in an explicit way. While De-Mixing task is an ill-posed problem, where a single mixed image corresponds to two different images (irrespective of order). Hence, we introduce a new loss function called Topological Consistency to train the model for De-Mixing in an implicit way. In the following sections, we will present the detailed discussion on the proposed method.

In-Image De-Folding

The patterns of face and fingerprint are quite different from that of the natural images. A typical case of the point is that the fingerprint and face perform a symmetric distribution in the global view of the images, but chirality in the local patterns, such as texture features and reflection. In the field of PAD, print photos, replay-videos and 3D masks are typical attacks for biometric recognition systems. Although the attacks are similar with the bona fide samples from the view of human vision, the texture of the attacks is generally unusual with anomalous reflection due to the specification of the instruments. As the features for PAD are mostly identical with the chiral features, a chirality-related pretext task, denoted as De-Folding is proposed in this paper.

As shown in Fig. 3, based on different modalities, we propose two strategies to fold images. In the case of face, a vertical line is adopted to cut the input image x_i into two patches, A_1 and A_2 , which are then randomly selected to flip horizontally to obtain A'_1 and A'_2 . Through resizing and averaging A'_1 and A'_2 , the folded image f_i , can be calculated, which is then drawn as the input of the following part. Unlike face, fingerprint shows chirality in both vertical and horizontal direction. Hence, x_i are cropped into four patches, $\{A_1, A_2, A_3, A_4\}$, by the vertical and horizontal lines. And the flips with various directions are correspondingly adopted to generate $\{A'_1, A'_2, A'_3, A'_4\}$. In order to improve the difficulty of the task and prevent the model from over fitting, the lines for cutting are randomly localized rather than frozen in the middle of image.

Since the paired data, i.e. (f_i, x_i) for De-Folding can be generated easily, the model is trained in an explicit way by maximizing cycle consistency. In particular, given f_i as input, a feature extractor $D(\cdot)$ is adopted to embed f_i into a latent representation z_i , while a generator $G(\cdot)$ is employed to reconstruct z_i to y_i . By following such cycle pipeline $x_i \rightarrow f_i \rightarrow y_i$, $D(\cdot)$ and $G(\cdot)$ are trained end-to-end by

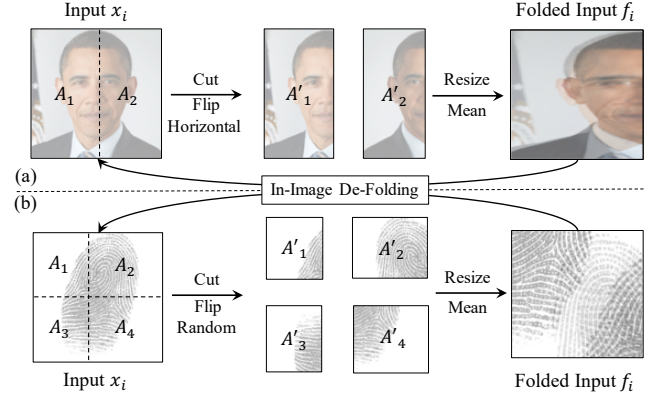


Figure 3: The pipeline of folding inputs in De-Folding task. (a) presents the case of face and (b) refers to the fingerprint case. The fingerprint sample is selected from LivDet2017 (Mura et al. 2018) and face is cropped from (Gecer et al. 2019).

the learning objective,

$$\begin{aligned} \min_{G, D} \quad & \mathcal{L}_r(y_i, x_i) + \mathcal{L}_g(y_j, x_i) \\ & \substack{x_i \sim \mathcal{X}_t \\ f_i \sim \mathcal{T}(\mathcal{X}_t)} \quad \substack{x_i \sim \mathcal{X}_t \\ f_j \sim \mathcal{T}(\mathcal{X}_t)} \\ \mathcal{L}_r(y_i, x_i) = & \mathbb{E}_{\substack{x_i \sim \mathcal{X}_t \\ f_i \sim \mathcal{T}(\mathcal{X}_t)}} \|y_i - x_i\|_2 \\ \mathcal{L}_g(y_j, x_i) = & \mathbb{E}_{\substack{x_i \sim \mathcal{X}_t \\ f_j \sim \mathcal{T}(\mathcal{X}_t)}} [F(x_i)] - \mathbb{E}_{f_j \sim \mathcal{T}(\mathcal{X}_t)} [F(y_j)] \end{aligned} \quad (1)$$

where $\mathcal{T}(\cdot)$ is the image folding and \mathcal{X}_t refers to the training set. $F(\cdot)$ is a discriminator, which has the same architecture with $D(\cdot)$ and is trained by maximizing \mathcal{L}_g . \mathcal{L}_r leads y_i to be similar with x_i in a supervised mode, while \mathcal{L}_g adopt the loss of WGAN (Arjovsky, Chintala, and Bottou 2017) to ensure the realness of y_i by following unsupervised setting.

Out-of-Image De-Mixing

Since De-Folding is an in-image task, the model leans to represent the images with region-specific features for reconstruction. Such pretext task pays more attention to the local patterns, but neglects the differences between the samples. As a result, varying samples can be embedded into the similar representations. However, PAD is a binary classification task, in which the ideal embedding space is compact but distinguishable for different samples. Therefore, in this paper, another pretext task, denoted as De-Mixing is proposed to further enhance the discrimination among the different samples. The model is not only required to reconstruct folded images but also disentangle mixed image from different samples. In De-Mixing task, two samples x_i and x_j are mixed into M_{ij} by

$$M_{ij} = \Delta_{\epsilon \sim \mathcal{U}(0,1)}(x_i, x_j) = \epsilon x_i + (1 - \epsilon) x_j \quad (2)$$

where $\mathcal{U}(0, 1)$ is the uniform distribution from 0. to 1., and ϵ is a scalar sampled from $\mathcal{U}(0, 1)$ for mixing. Given M_{ij}

as input, the feature extractor $D(\cdot)$ is required to disentangle M_{ij} into x_i and x_j . However, such a requirement draws the task as an ill-posed problem, which is hard to train end-to-end. Considering the groundtruth of De-Mixing, both $\{x_i, x_j\}$ and $\{x_j, x_i\}$ are the correct results. But for $D(\cdot)$, the order changing in the groundtruth is regarded as different labels. To overcome the problem, De-Mixing task is trained in an implicit way using topological consistency \mathcal{L}_t ,

$$\mathcal{L}_t(x_i, x_j) = \mathbb{E}_{x_i, x_j \sim \mathcal{X}_t} \|z_{ij} - \hat{z}_{ij} + \delta\|_2 \quad (3)$$

$$\hat{z}_{ij} = \Delta(z_i, z_j)$$

where ϵ for M_{ij} and \hat{z}_{ij} is identical, z_i, z_j and z_{ij} are the outputs of $D(x_i), D(x_j)$ and $D(M_{ij})$ respectively and δ is a random noise sampled from a Gaussian distribution with 0. mean and 0.1 standard deviation. By minimizing the distance between z_{ij} and \hat{z}_{ij} , the mixing operation is identical in both image and embedding space. Since $\{z_i, z_j, z_{ij}\}$ has the same topological structure with $\{x_i, x_j, M_{ij}\}$, M_{ij} can be de-mixed easily in the embedding space of $D(\cdot)$, which approximately meets the target of De-Mixing. Note that topological consistency has trivial solution, e.g. embedding the same code for all images, $\delta \in \mathcal{N}(0, 0.1)$ is thus added into \mathcal{L}_t to enhance the gradients against collapsing cases.

IF-OM based Presentation Attack Detection

Considering the complementarity between De-Folding and De-Mixing, the proposed method trains $D(\cdot)$ with both pre-text tasks simultaneously, and the total learning objective can be concluded as

$$\min_{G, D} \mathcal{L}_r(y_i, x_i) + \mathcal{L}_g(y_j, x_i) + \mathcal{L}_t(x_i, x_j) \quad (4)$$

$$f_i \sim \mathcal{T}(\mathcal{X}_t) \quad x_i \sim \mathcal{X}_t \quad x_j \sim \mathcal{X}_t \quad f_j \sim \mathcal{T}(\mathcal{X}_t)$$

After training, $D(\cdot)$ is employed as the initialization for a presentation attack detector $H(\cdot)$. Compared with $D(\cdot)$, $H(\cdot)$ has an additional fully-connected layer to map z_i into a single scalar v_i , i.e spoofness score. Spoofness score reflects the category probability (PA or not) of the given sample x_i . $H(\cdot)$ is trained through a common cross entropy based objective as follow:

$$\mathcal{L}_c(x_i, v_i) = - \mathbb{E}_{x_i \in \mathcal{X}_t} [u_i \log(v_i) + (1 - u_i) \log(1 - v_i)] \quad (5)$$

where $v_i = H(x_i)$ and u_i is the category annotation of x_i . For clarity, the proposed method is summarized in Algo. 1.

Experimental Results and Analysis

To evaluate the performance of the proposed method, extensive experiments are carried on the publicly-available datasets, including LivDet2017(Mura et al. 2018), OULU-NPU (Boulkenafet et al. 2017), CASIA-FASD (Zhang et al. 2012), Idiap Replay-Attack (Chingovska, Anjos, and Marcel 2012) and MSU-MFSD (Wen, Han, and Jain 2015). We first introduce the datasets and the corresponding implementation details. Then, the effectiveness of the proposed method is validated by analyzing the contribution of each component. Since this is the first time to adopt self-supervised

Algorithm 1: Presentation Attack Detection using IF-OM

Input:

Feature Extractor $D(\cdot)$; Generator $G(\cdot)$; Discriminator $F(\cdot)$; Training Set \mathcal{X}_t ; Presentation Attack Detector $H(\cdot)$;

Output:

Trained $H(\cdot)$;

```

1: while  $D(\cdot)$  has not converged do
2:   for  $x_i, x_j$  in  $\mathcal{X}_t$  do
3:     Derive folded input  $f_i$  from  $\mathcal{T}(x_i)$ ;
4:     Reconstruct  $f_i$  to  $y_i$  through  $G(D(f_i))$ ;
5:     Update  $G(\cdot)$  and  $D(\cdot)$  by minimizing Eq.(1);
6:     Update  $F(\cdot)$  by maximizing  $\mathcal{L}_g$ ;
7:     Calculate  $M_{ij}$  from  $x_i$  and  $x_j$  through Eq.(2);
8:     Update  $D(\cdot)$  by minimizing Eq.(3)
9:   end for
10: end while
11: while  $H(\cdot)$  has not converged do
12:   Adopt  $D(\cdot)$  as the initialization of  $H(\cdot)$ ;
13:   for  $x_i$  in  $\mathcal{X}_t$  do
14:     Obtain spoofness score  $v_i$  by  $H(x_i)$ ;
15:     Update  $H(\cdot)$  by minimizing Eq.(5);
16:   end for
17: end while
18: Return  $H(\cdot)$ ;
```

learning for PAD, we finally compare the proposed method with both existing self-supervised methods and PA detectors to further prove the superiority of the proposed method.

Datasets and Implementation Details

As the proposed method is evaluated in two modalities, including fingerprint and face, we separately introduce the details of the corresponding protocols as follows:

Fingerprint. Due to the complete experimental settings, LivDet 2017 (Mura et al. 2018) is used to test the methods on fingerprint PAD. The dataset is composed of over 17,500 fingerprint images captured from three different readers, i.e., Green Bit, Orcanhus and Digital Persona. For each sensor, about 1760 fingerprint images are used for training, 440 images for validation and 3740 images for testing. To evaluate the generalization of the competing methods, cross-material and cross-sensor settings (Liu et al. 2021b) are used in this paper. For cross-material case, the spoof materials available in test set are deemed as unknown material, which are inaccessible during training. The partition of materials follows the setting in (Liu et al. 2021b). In the cross-sensor protocol, PA detectors are trained by the images collected using a randomly-selected sensor, and then tested using the images from the other sensors. Equal Error Rate (EER), Area Under Curve (AUC) and true detection rate (TDR) @ false detection rate (FDR)=1% are used to evaluate the performance of detection.

In terms of network architecture, MobileNet V2 (Sandler et al. 2018) is selected as the backbone for the feature extractor and discriminator, while the corresponding generator is designed by following U-Net architecture (Ronneberger,

Baseline	In-Image De-Folding	Out-of-Image De-Mixing	GreenBit			DigitalPersona			Oranthur			Mean \pm s.d.		
			EER(%)	AUC(%)	TDR(%)	EER(%)	AUC(%)	TDR(%)	EER(%)	AUC(%)	TDR(%)	EER(%)	AUC(%)	TDR(%)
✓	×	×	3.99	99.13	81.67	5.08	98.80	68.64	3.23	99.24	71.46	4.10 \pm 0.93	99.06 \pm 0.23	73.92 \pm 6.86
✓	✓	×	3.17	99.38	86.01	3.90	99.03	72.78	2.88	99.24	77.45	3.32 \pm 0.53	99.22 \pm 0.18	78.75 \pm 6.71
✓	×	✓	3.58	99.19	84.95	3.44	99.14	74.56	2.66	99.61	90.98	3.23 \pm 0.50	99.31 \pm 0.26	83.50 \pm 8.31
✓	✓	✓	2.88	99.65	94.14	3.49	99.26	81.36	1.40	99.75	97.37	2.59 \pm 1.07	99.55 \pm 0.26	90.96 \pm 8.47

Table 1: Performance of the Proposed Method with or without Each Component in the terms of EER (%) \downarrow , AUC (%) \uparrow and TDR(%)@FDR=1.0% \uparrow under the Cross-Material Setting on LivDet2017.

Baseline	In-Image De-Folding	Out-of-Image De-Mixing	[O,M] to [C, I]			[C,I] to [O, M]			Mean \pm s.d.		
			EER(%)	AUC(%)	TDR(%)	EER(%)	AUC(%)	TDR(%)	EER(%)	AUC(%)	TDR(%)
✓	×	×	25.65	79.14	4.07	28.14	79.05	18.66	26.90 \pm 1.76	79.10 \pm 0.06	11.37 \pm 10.32
✓	✓	×	20.33	84.51	9.79	25.38	81.16	26.70	22.86 \pm 3.57	82.84 \pm 2.37	18.25 \pm 11.96
✓	×	✓	21.07	85.17	11.93	26.33	80.25	27.49	23.70 \pm 3.72	82.71 \pm 3.48	19.71 \pm 11.00
✓	✓	✓	18.96	89.48	30.48	18.60	89.76	30.30	18.78 \pm 0.25	89.62 \pm 0.20	30.39 \pm 0.13

Table 2: Performance of the Proposed Method with or without Each Component in the terms of EER (%) \downarrow , AUC (%) \uparrow and TDR(%)@FDR=1.0% \uparrow under the Cross-Dataset Setting on OULU-NPU (O), CAISIA-FASD (C), Idiap Replay-Attack (I) and MSU-MFSD (M).

Fischer, and Brox 2015). The model is trained by Adam with $\beta_1 = 0.9$ and $\beta_2 = 0.999$. The learning rate is $1e-6$ with $5e-4$ weight decay. Batch size for training is 12. When comes to training PA detector based on the proposed method, the batch size is set as 128, learning rate refers to $1e-4$ and the other parameters are identical with IF-OM. Note that, in order to test the capacity of feature extraction and reduce the dependence on data scale, only the training set adopted for PAD is drawn to train the proposed method.

We compare the proposed method with both self-supervised learning based methods and presentation attack detectors. For self-supervised learning based methods, GAN based discriminator (Isola et al. 2017) and auto-encoder based encoder (Isola et al. 2017) are set as the baseline of the generative learning, while MoCo V2 (Chen et al. 2020b) is selected as the representative method of the contrastive learning. In the terms of PA detector, LivDet 2017 winner (Mura et al. 2018) and FSB (Chugh, Cao, and Jain 2018) are adopted as the competing method. For more comprehensive analysis on the proposed method, multiple models based PA detectors, including RTK-PAD (Liu et al. 2021b) and FSB + UMG Wrapper (Chugh and Jain 2021) are also included for reference.

Face. To test the performance of face PAD, 4 datasets including OULU-NPU (Boulkenafet et al. 2017) (denoted as O), CASIA-FASD (Zhang et al. 2012) (denoted as C), Idiap Replay-Attack (Chingovska, Anjos, and Marcel 2012) (denoted as I) and MSU-MFSD (Wen, Han, and Jain 2015) (denoted as M) are adopted in this paper for evaluation using a cross-dataset protocol. In particular, [O,M] and [C,I] are set as two groups. The model is trained in one group and tested in the other.

In this case, MTCNN algorithm (Zhang et al. 2016) is adopted for face detection and alignment. All the detected faces are resized to (256,256). ResNet18 (He et al. 2016) is set as the backbone for the feature extractor and discriminator. The model is trained with 32 batch size by Adam optimizer ($\beta_1 = 0.9, \beta_2 = 0.999$). The learning rate is $1e-4$ and the weight decay is $5e-4$. For PAD, the feature extractor is

	Fingerprint			Face		
	EER(%)	AUC(%)	TDR(%)	EER(%)	AUC(%)	TDR(%)
Baseline	13.26	93.46	29.28	42.30	59.51	4.14
GAN based Discriminator	12.59	93.66	34.33	38.99	63.38	4.34
AE based Encoder	11.20	94.83	27.78	35.65	65.79	2.70
MoCo V2	20.87	86.18	13.10	40.77	64.58	6.04
Ours: IF-OM	8.87	96.55	56.42	31.28	73.68	10.06
Pre-Trained from ImageNet	4.10	99.06	73.92	26.90	79.10	11.37
Ours: IF-OM (ImageNet)	2.59	99.55	90.96	18.78	89.62	30.39

More details of the results in each case are given in the appendix.

Table 3: Performance Comparison between the Proposed Method and Self-Supervised Methods in the Terms of EER(%) \downarrow , AUC(%) \uparrow and TDR(%)@FDR=1.0% \uparrow under the Cross-Material Setting on LivDet2017 and the Cross-Dataset Setting on [O, M] and [C, I].

fine-tuned by SGD with $1e-2$ learning rate, 0.9 momentum and $5e-4$ weight decay.

Besides the mentioned self-supervised methods, the state-of-the-art PA detectors, including DeepPixBiS (George and Marcel 2019), SSDG-R (Jia et al. 2020), CDC (Yu et al. 2020) are conducted in this paper. The effectiveness is validated by the improvement of such methods adopting the proposed method as initialization.

This paper adopts the public platform pytorch for all experiments using a work station with CPUs of 2.8GHz, RAM of 512GB and GPUs of NVIDIA Tesla V100.

Effectiveness Analysis of the Proposed Method

To quantify the contribution of Out-of-Image De-Mixing and In-Image De-Folding, we test the performance of PAD with or without the corresponding pretext task. Table 1 and Table 2 show the results carried on fingerprint and face cases respectively. The baseline is set as the model pre-trained from ImageNet for PAD. Compared with the baseline, both De-Folding and De-Mixing can provide more reasonable initialization. Specifically, an increase of 9.58% in mean TDR@FDR=1.0% is achieved by adopting De-Mixing as the pretext task in Table 1. When it comes to face, De-Folding improves the EER of baseline from 26.90% to 22.86%. This indicates that both components in the pro-

		Cross-Material Case		Cross-Sensor Case		Mean	
		ACE(%)	TDR(%)	ACE(%)	TDR(%)	ACE(%)	TDR(%)
Single Model	LivDet 2017 Winner	4.75 ± 1.40	-	-	-	-	-
	F.S.B.	4.56 ± 1.12	73.32 ± 15.52	32.40 ± 16.92	21.26 ± 28.06	18.48	50.69
	Ours: IF-OM	2.48 ± 0.98	90.96 ± 8.47	19.82 ± 9.80	33.43 ± 24.12	11.15	62.20
Multiple Models (Ensemble Learning)	F.S.B. + UMG Wrapper	4.12 ± 1.34	80.74 ± 10.02	20.37 ± 12.88	43.23 ± 28.31	12.25	61.99
	RTK-PAD	2.12 ± 0.72	91.20 ± 7.59	21.87 ± 10.48	34.70 ± 25.30	12.00	62.95

The competing methods only report the result in ACE and TDR@FDR=1.0%, we thus test the proposed method in ACE.
More details of the results in each case are given in the appendix.

Table 4: Performance Comparison between the Proposed Method and the State-Of-The-Art Methods on LivDet2017 under the Cross-Material and Cross-Sensor Settings in the Terms of Average Class Error (%) ↓ and TDR(%)@FDR=1.0% ↑.

	[O,M] to [C, I]			[C,I] to [O, M]			Mean ± s.d.		
	EER(%)	AUC(%)	TDR(%)	EER(%)	AUC(%)	TDR(%)	EER(%)	AUC(%)	TDR(%)
Baseline: DeepPixBiS	22.93	79.13	0.00	22.45	85.70	24.37	22.69 ± 0.34	82.42 ± 4.65	12.19 ± 17.23
Ours: DeepPixBiS + IF-OM	15.94	92.60	42.34	22.14	86.36	34.08	19.04 ± 4.38	89.48 ± 4.41	38.21 ± 5.84
Baseline: SSDG-R	20.92	88.07	9.72	22.57	85.61	15.95	21.75 ± 1.17	86.84 ± 1.74	12.84 ± 4.41
Ours: SSDG-R + IF-OM	18.60	88.80	15.52	18.92	88.59	47.90	18.76 ± 0.23	88.70 ± 0.15	31.71 ± 22.90
Baseline: CDC	28.94	78.96	13.93	23.30	83.42	25.83	26.12 ± 3.99	81.19 ± 3.15	19.88 ± 8.41
Ours: CDC + IF-OM	26.00	81.73	14.76	21.86	85.77	34.95	23.93 ± 2.93	83.75 ± 2.86	24.86 ± 14.28

* This paper adopts ResNet-18 as the backbone for CDC.

Table 5: Performance of Various PAD Methods with or without the Proposed Method as Initialization in the Terms of EER(%) ↓, AUC(%) ↑ and TDR(%)@FDR=1.0% ↑ under the Cross-Dataset Setting of Face.

posed method can promote PAD effectively. Among all the cases, the most significant improvement is obtained when all the designed components are adopted, i.e. IF-OM can reach to 18.78% and 2.59% mean EER in face and fingerprint respectively, which significantly outperforms those of baseline.

Comparison with Related Methods

Comparison with Self-Supervised Methods Due to the difference between the natural and face/fingerprint images, directly adopting existing self-supervised methods for PAD is not a proper choice. To our best knowledge, this is the first time to employ a specific self-supervised method for PAD. To validate the effectiveness of the proposed method, we compare IF-OM with the existing self-supervised methods. As the results listed in Table 3, the proposed method outperforms existing methods significantly. In terms of face, when trained from scratch, our method can achieve an EER of 31.28%, exceeding other self-supervised methods by around 4~10 % absolutely. Meanwhile, the proposed method can further improve the performance of the model pre-trained from ImageNet. Typically, in the case of fingerprint, IF-OM reaches 90.96% TDR when FDR=1.0%, which outperforms the initialization from ImageNet in a large margin, i.e. 90.96% vs. 73.92%. Note that the data scale of PAD is limited, hence, contrastive learning can not reach to competitive results and may lead model to learn useful features for identification but useless for PAD.

Comparison with Presentation Attack Detectors To further verify the effectiveness of the proposed method, we compare it with the state-of-the-art methods. As the results listed in Table 4, under the cross-material and cross-sensor settings, the proposed method can outperform other single model based methods by a large margin. In the cross-sensor

case, compared with FSB, a reduction of 12.58% in average classification error (ACE) can be obtained by IF-OM. By comprehensively analyzing cross-material and -sensor protocols, IF-OM can promote PA detector to 11.15% mean ACE, even exceeding the multiple model based methods, which convincingly proves the advantage of IF-OM.

When comes to face, we re-implement some famous PA detectors and investigate the improvement from IF-OM in different detectors. As listed in Table 5, IF-OM can facilitate the performance of detection by around 5~25% in mean TDR@FDR=1.0%. When DeepPixBiS is used as the detector, IF-OM can improve the AUC of PAD from 82.42% to 89.48%. The experimental results indicate that the proposed method is general and can be integrated with various PA detectors.

Conclusion

In this paper, we proposed a self-supervised learning based method to improve the generalization performance of PA detectors. De-Folding and De-Mixing pretext tasks included in the method work together as a local-global strategy. That is, De-Folding requires the model to reconstruct the folded image to the row by extracting region-specific features, i.e. local information, while De-Mixing drives the model to derive instance-specific features, i.e. global information, by disentangling the mixed samples. The generalization ability is finally improved by the comprehensive local-global view on training samples. The effectiveness of the proposed method is verified in terms of face and fingerprint PAD, including 5 publicly-available datasets: LivDet2017, OULU-NPU, CASIA-FASD, Idiap Replay-Attack and MSU-MFSD. In the future, we will further investigate the application of the proposed method in other tasks, such as fingerprint/face recognition and face detection/alignment.

Acknowledgment

The work is partially supported by the National Natural Science Foundation of China under grants no. 62076163 and 91959108, the Shenzhen Fundamental Research fund JCYJ20190808163401646, JCYJ20180305125822769, Tencent “Rhinoceros Birds”-Scientific Research Foundation for Young Teachers of Shenzhen University and the Research Council of Norway (No. 321619 Project “OffPAD”).

References

- Arjovsky, M.; Chintala, S.; and Bottou, L. 2017. Wasserstein generative adversarial networks. In *International conference on machine learning*, 214–223. PMLR.
- Boulkenafet, Z.; Komulainen, J.; and Hadid, A. 2016. Face antispoofing using speeded-up robust features and fisher vector encoding. *IEEE Signal Processing Letters*, 24(2): 141–145.
- Boulkenafet, Z.; Komulainen, J.; Li, L.; Feng, X.; and Hadid, A. 2017. Oulu-npu: A mobile face presentation attack database with real-world variations. In *2017 12th IEEE international conference on automatic face & gesture recognition (FG 2017)*, 612–618. IEEE.
- Chen, T.; Kornblith, S.; Norouzi, M.; and Hinton, G. 2020a. A simple framework for contrastive learning of visual representations. In *International conference on machine learning*, 1597–1607. PMLR.
- Chen, X.; Fan, H.; Girshick, R.; and He, K. 2020b. Improved baselines with momentum contrastive learning. *arXiv preprint arXiv:2003.04297*.
- Chingovska, I.; Anjos, A.; and Marcel, S. 2012. On the effectiveness of local binary patterns in face anti-spoofing. In *2012 BIOSIG-proceedings of the international conference of biometrics special interest group (BIOSIG)*, 1–7. IEEE.
- Chugh, T.; Cao, K.; and Jain, A. K. 2018. Fingerprint Spoof Buster: Use of Minutiae-Centered Patches. *IEEE Transactions on Information Forensics and Security*, 13(9): 2190–2202.
- Chugh, T.; and Jain, A. K. 2021. Fingerprint Spoof Detector Generalization. *IEEE Transactions on Information Forensics and Security*, 16: 42–55.
- de Freitas Pereira, T.; Anjos, A.; De Martino, J. M.; and Marcel, S. 2013. Can face anti-spoofing countermeasures work in a real world scenario? In *2013 international conference on biometrics (ICB)*, 1–8. IEEE.
- Doersch, C.; Gupta, A.; and Efros, A. A. 2015. Unsupervised visual representation learning by context prediction. In *Proceedings of the IEEE international conference on computer vision*, 1422–1430.
- Gecer, B.; Ploumpis, S.; Kotsia, I.; and Zafeiriou, S. 2019. Ganfit: Generative adversarial network fitting for high fidelity 3d face reconstruction. In *Proceedings of the IEEE/CVF Conference on Computer Vision and Pattern Recognition*, 1155–1164.
- George, A.; and Marcel, S. 2019. Deep pixel-wise binary supervision for face presentation attack detection. In *2019 International Conference on Biometrics (ICB)*, 1–8. IEEE.
- George, A.; and Marcel, S. 2020. Learning one class representations for face presentation attack detection using multi-channel convolutional neural networks. *IEEE Transactions on Information Forensics and Security*, 16: 361–375.
- Gidaris, S.; Singh, P.; and Komodakis, N. 2018. Unsupervised representation learning by predicting image rotations. *arXiv preprint arXiv:1803.07728*.
- Goodfellow, I.; Pouget-Abadie, J.; Mirza, M.; Xu, B.; Warde-Farley, D.; Ozair, S.; Courville, A.; and Bengio, Y. 2014. Generative adversarial nets. *Advances in neural information processing systems*, 27.
- Grill, J.-B.; Strub, F.; Altché, F.; Tallec, C.; Richemond, P. H.; Buchatskaya, E.; Doersch, C.; Pires, B. A.; Guo, Z. D.; Azar, M. G.; et al. 2020. Bootstrap your own latent: A new approach to self-supervised learning. *arXiv preprint arXiv:2006.07733*.
- Guo, J.; Zhu, X.; Xiao, J.; Lei, Z.; Wan, G.; and Li, S. Z. 2019. Improving face anti-spoofing by 3d virtual synthesis. In *2019 International Conference on Biometrics (ICB)*, 1–8. IEEE.
- He, K.; Fan, H.; Wu, Y.; Xie, S.; and Girshick, R. 2020. Momentum contrast for unsupervised visual representation learning. In *Proceedings of the IEEE/CVF Conference on Computer Vision and Pattern Recognition*, 9729–9738.
- He, K.; Zhang, X.; Ren, S.; and Sun, J. 2016. Deep Residual Learning for Image Recognition. In *Proceedings of the IEEE Conference on Computer Vision and Pattern Recognition (CVPR)*.
- Heusch, G.; George, A.; Geissbühler, D.; Mostaani, Z.; and Marcel, S. 2020. Deep models and shortwave infrared information to detect face presentation attacks. *IEEE Transactions on Biometrics, Behavior, and Identity Science*, 2(4): 399–409.
- Isola, P.; Zhu, J.-Y.; Zhou, T.; and Efros, A. A. 2017. Image-to-image translation with conditional adversarial networks. In *Proceedings of the IEEE conference on computer vision and pattern recognition*, 1125–1134.
- Jia, Y.; Zhang, J.; Shan, S.; and Chen, X. 2020. Single-side domain generalization for face anti-spoofing. In *Proceedings of the IEEE/CVF Conference on Computer Vision and Pattern Recognition*, 8484–8493.
- Jing, L.; and Tian, Y. 2020. Self-supervised visual feature learning with deep neural networks: A survey. *IEEE transactions on pattern analysis and machine intelligence*.
- Larbi, K.; Ouada, W.; Drira, H.; Ben Amor, B.; and Ben Amar, C. 2018. DeepColorFASD: Face Anti Spoofing Solution Using a Multi Channeled Color Spaces CNN. In *2018 IEEE International Conference on Systems, Man, and Cybernetics (SMC)*, 4011–4016.
- Ledig, C.; Theis, L.; Huszár, F.; Caballero, J.; Cunningham, A.; Acosta, A.; Aitken, A.; Tejani, A.; Totz, J.; Wang, Z.; et al. 2017. Photo-realistic single image super-resolution using a generative adversarial network. In *Proceedings of the IEEE conference on computer vision and pattern recognition*, 4681–4690.

- Liu, F.; Liu, H.; Zhang, W.; Liu, G.; and Shen, L. 2021a. One-Class Fingerprint Presentation Attack Detection Using Auto-Encoder Network. *IEEE Transactions on Image Processing*, 30: 2394–2407.
- Liu, H.; Zhang, W.; Liu, F.; Wu, H.; and Shen, L. 2021b. Fingerprint Presentation Attack Detector Using Global-Local Model. *IEEE Transactions on Cybernetics*, 1–14.
- Liu, Y.; Jourabloo, A.; and Liu, X. 2018. Learning deep models for face anti-spoofing: Binary or auxiliary supervision. In *Proceedings of the IEEE conference on computer vision and pattern recognition*, 389–398.
- Liu, Y.; Stehouwer, J.; Jourabloo, A.; and Liu, X. 2019. Deep tree learning for zero-shot face anti-spoofing. In *Proceedings of the IEEE/CVF Conference on Computer Vision and Pattern Recognition*, 4680–4689.
- Mura, V.; Orrù, G.; Casula, R.; Sibiri, A.; Loi, G.; Tuveri, P.; Ghiani, L.; and Marcialis, G. L. 2018. LivDet 2017 fingerprint liveness detection competition 2017. In *2018 International Conference on Biometrics (ICB)*, 297–302. IEEE.
- Patel, K.; Han, H.; and Jain, A. K. 2016. Secure face unlock: Spoof detection on smartphones. *IEEE transactions on information forensics and security*, 11(10): 2268–2283.
- Pathak, D.; Krahenbuhl, P.; Donahue, J.; Darrell, T.; and Efros, A. A. 2016. Context encoders: Feature learning by inpainting. In *Proceedings of the IEEE conference on computer vision and pattern recognition*, 2536–2544.
- Raghavendra, R.; Raja, K. B.; and Busch, C. 2015. Presentation Attack Detection for Face Recognition Using Light Field Camera. *IEEE Transactions on Image Processing*, 24(3): 1060–1075.
- Ramachandra, R.; and Busch, C. 2017. Presentation attack detection methods for face recognition systems: A comprehensive survey. *ACM Computing Surveys (CSUR)*, 50(1): 1–37.
- Ronneberger, O.; Fischer, P.; and Brox, T. 2015. U-net: Convolutional networks for biomedical image segmentation. In *International Conference on Medical image computing and computer-assisted intervention*, 234–241. Springer.
- Russakovsky, O.; Deng, J.; Su, H.; Krause, J.; Satheesh, S.; Ma, S.; Huang, Z.; Karpathy, A.; Khosla, A.; Bernstein, M.; et al. 2015. Imagenet large scale visual recognition challenge. *International journal of computer vision*, 115(3): 211–252.
- Sandler, M.; Howard, A.; Zhu, M.; Zhmoginov, A.; and Chen, L.-C. 2018. Mobilenetv2: Inverted residuals and linear bottlenecks. In *Proceedings of the IEEE conference on computer vision and pattern recognition*, 4510–4520.
- Singh, J. M.; Madhun, A.; Li, G.; and Ramachandra, R. 2020. A survey on unknown presentation attack detection for fingerprint. *arXiv preprint arXiv:2005.08337*.
- Wang, G.; Han, H.; Shan, S.; and Chen, X. 2020. Cross-domain face presentation attack detection via multi-domain disentangled representation learning. In *Proceedings of the IEEE/CVF Conference on Computer Vision and Pattern Recognition*, 6678–6687.
- Wang, Y.; Song, X.; Xu, T.; Feng, Z.; and Wu, X.-J. 2021. From RGB to Depth: Domain Transfer Network for Face Anti-Spoofing. *IEEE Transactions on Information Forensics and Security*.
- Wen, D.; Han, H.; and Jain, A. K. 2015. Face spoof detection with image distortion analysis. *IEEE Transactions on Information Forensics and Security*, 10(4): 746–761.
- Yang, J.; Lei, Z.; Liao, S.; and Li, S. Z. 2013. Face liveness detection with component dependent descriptor. In *2013 International Conference on Biometrics (ICB)*, 1–6. IEEE.
- Yu, Z.; Zhao, C.; Wang, Z.; Qin, Y.; Su, Z.; Li, X.; Zhou, F.; and Zhao, G. 2020. Searching central difference convolutional networks for face anti-spoofing. In *Proceedings of the IEEE/CVF Conference on Computer Vision and Pattern Recognition*, 5295–5305.
- Zhang, K.; Zhang, Z.; Li, Z.; and Qiao, Y. 2016. Joint face detection and alignment using multitask cascaded convolutional networks. *IEEE Signal Processing Letters*, 23(10): 1499–1503.
- Zhang, R.; Isola, P.; and Efros, A. A. 2016. Colorful image colorization. In *European conference on computer vision*, 649–666. Springer.
- Zhang, Z.; Yan, J.; Liu, S.; Lei, Z.; Yi, D.; and Li, S. Z. 2012. A face antispoofing database with diverse attacks. In *2012 5th IAPR international conference on Biometrics (ICB)*, 26–31. IEEE.
- Zhu, J.-Y.; Park, T.; Isola, P.; and Efros, A. A. 2017. Unpaired image-to-image translation using cycle-consistent adversarial networks. In *Proceedings of the IEEE international conference on computer vision*, 2223–2232.

Appendix

Details of the Datasets

To clarify our experimental settings, we give the details of the datasets in this section. Table A.1 summarizes the information of LivDet2017, which is used to evaluate the performance of fingerprint PAD. LivDet 2017 consists of over 17500 fingerprint images, captured from GreenBit, Orcanthus and Digital Persona. Specifically, GreenBit is employed for Italian border controls and issuance of Italian electronic documents. Orcanthus is widely used in the personal computer (PC). And Digital Persona is adopted in the mobile devices, such as Nexus 7 tablet. Hence, the adopted readers are reliable to test the practical performance for fingerprint PAD. More details are available at Table A.1.

TABLE A. 1. Details of LivDet2017 Datasets.

Fingerprint Reader	GreenBit DactyScan84c	Orcanthus Certis2 Imag	Digital Persona U.are.U 5160
Type	Optical	Thermal swipe	Optical
Application	Italian Border Control	Personal Computer	Nexus 7 Tablet
Image Size(w×h)	500 × 500	-*	252 × 324
Resolution(dpi)	500	500	500
Live Image(Train/Test)	1000/1700	1000/1700	999/1700
Spoof Images(Train/Test)	1200/2040	1200/2018	1199/2028
Spoof Materials for Training	Wood Glue, Exoflex, Body Double		
Spoof Materials for Testing	Gelatine, Liquid Ecoflex, Latex		

* The images derived from Orcanthus reader are with the variable size.

Meanwhile, we conclude the information for the datasets with respect to face PAD. As listed in Table A. 2, four datasets, including Oulu-NPU, CASIA-FASD, Idiap Replay-Attack and MSU-MFSD, are used to evaluate the performance of PAD in this paper. In particular, printed photos, display photos and replayed videos are adopted as the attacks for facial recognition system. Various acquisition devices, such as laptop and smartphone, are considered in different datasets. Hence the robustness and generalization of the PAD methods can be tested through cross-dataset protocol. In such protocol, [O,M] and [C,I] are set as two different groups. The model is trained on a given group and tested on the other one. For each video, only one randomly-selected frame is used to train or test the detectors.

TABLE A. 2. Summary of Oulu-NPU, CASIA-FASD, Idiap Replay-Attack and MSU-MFSD.

	Attack type	Subject		videos		Acquisition devices	Display devices
		train	test	real	attack		
Oulu-NPU (O)	Printed photo Display photo Replayed video	35	20	1980	3960	6 smartphone	Dell 1950FP Macbook Retina
CASIA-FASD (C)	Printed photo Cut photo Replayed video	20	30	150	450	3 webcams	iPad
Idiap Replay-Attack (I)	Printed photo Replay video	30	20	390	640	1 laptop	iPhone 3GS iPad
MSU-MFSD (M)	Printed photo Cut photo Replayed video	18	17	110	330	1 laptop 1 smartphone	iPad Air iphone 5s

Ablation Study

To quantify the contribution of Out-of-Image De-Mixing and In-Image De-Folding, we test the discriminative performance of the variants with or without each pretext tasks. Fig. A.1 shows the ROC curves carried on fingerprint and face cases respectively, which is corresponding to Table 1 and Table 2 in the main body. As shown in Fig. A.1, the first row refers to the fingerprint case on LivDet2017 and the second row is the face case on Oulu-NPU, CASIA-FASD, Idiap and MSU-MFSD. The proposed method with blue line shows distinct advance over the other baselines among all the cases.

Comparison with Self-Supervised Methods

To prove the superiority of the proposed method, we compare IF-OM with other self-supervised learning based methods, including GAN based Discriminator, AE based Encoder and MoCo V2. The averaging performance is presented in the Table.

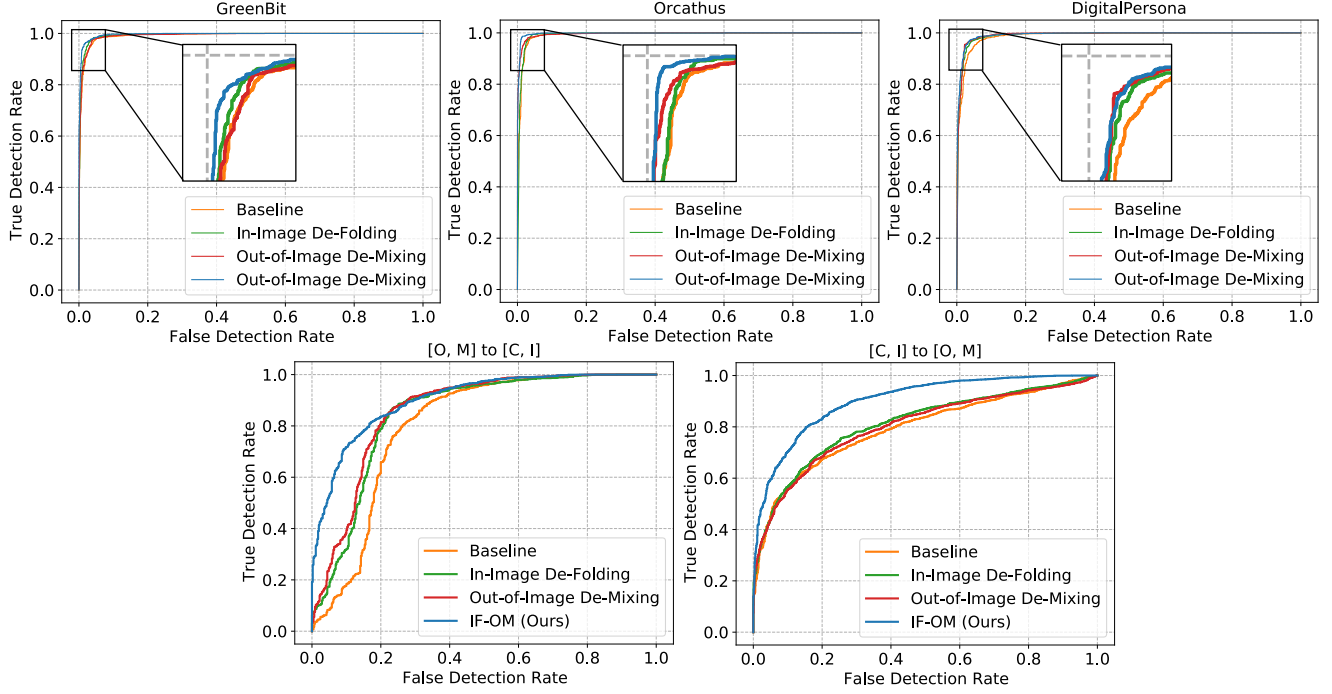


Figure A. 1. ROC curves for the ablation study. The first row presents the cases on LivDet2017 under the cross-material setting. The second row refers to the face anti-spoofing under the cross-dataset setting on [O,M] and [C,I].

TABLE A. 3. Performance Comparison between the Proposed Method and the Self-Supervised Methods on LivDet2017 under the Cross-Material Setting in the Terms of EER(%) \downarrow , AUC(%) \uparrow and TDR(%)@FDR=1.0% \uparrow .

	GreenBit			DigitalPersona			Oranthus			Mean \pm s.d.		
	EER(%)	AUC(%)	TDR(%)	EER(%)	AUC(%)	TDR(%)	EER(%)	AUC(%)	TDR(%)	EER(%)	AUC(%)	TDR(%)
Baseline	10.66	96.20	41.97	15.24	92.12	40.43	13.88	92.06	5.45	13.26 \pm 2.35	93.46 \pm 2.37	29.28 \pm 20.65
GAN based Discriminator	9.33	96.03	40.86	12.34	94.07	51.33	16.11	90.88	10.80	12.59 \pm 3.40	93.66 \pm 2.60	34.33 \pm 21.04
AE based Encoder	7.98	97.31	47.27	12.29	94.64	31.51	13.34	92.55	4.56	11.20 \pm 2.84	94.83 \pm 3.39	27.78 \pm 21.60
MoCo V2	18.39	88.67	14.15	24.41	83.67	17.03	19.82	86.20	8.13	20.87 \pm 3.15	86.18 \pm 2.50	13.10 \pm 4.54
Ours: IF-OM	7.68	97.61	59.14	9.27	96.54	68.20	9.66	95.51	41.92	8.87 \pm 1.05	96.55 \pm 1.05	56.42 \pm 13.35
Pre-Trained from ImageNet	3.99	99.13	81.67	5.08	98.80	68.64	3.23	99.24	71.46	4.10 \pm 0.93	99.06 \pm 0.23	73.92 \pm 6.86
Ours: IF-OM (ImageNet)	2.88	99.65	94.14	3.49	99.26	81.36	1.40	99.75	97.37	2.59 \pm 1.07	99.55 \pm 0.26	90.96 \pm 8.47

TABLE A. 4. Performance Comparison between the Proposed Method and the Self-Supervised Methods under the Cross-Dataset Setting on Oulu-NPU (O), CASIA-FASD (C), Idiap Replay-Attack(I) and MSU-MFSD (M) in the Terms of EER(%) \downarrow , AUC(%) \uparrow and TDR(%)@FDR=1.0% \uparrow .

	[O,M] to [C, I]			[C,I] to [O, M]			Mean \pm s.d.		
	EER(%)	AUC(%)	TDR(%)	EER(%)	AUC(%)	TDR(%)	EER(%)	AUC(%)	TDR(%)
Baseline	37.50	64.65	2.21	47.10	54.36	6.07	42.30 \pm 6.79	59.51 \pm 7.28	4.14 \pm 2.73
Gan based Discriminator	36.39	65.02	0.14	41.59	61.73	8.54	38.99 \pm 3.68	63.38 \pm 2.33	4.34 \pm 5.94
AE based Encoder	32.25	67.72	0.34	39.05	63.86	5.06	35.65 \pm 4.81	65.79 \pm 2.73	2.70 \pm 3.34
MoCo V2	33.75	68.00	0.00	47.79	61.16	12.07	40.77 \pm 9.93	64.58 \pm 4.84	6.04 \pm 8.53
Ours: IF-OM	29.61	73.78	6.76	32.94	73.58	13.36	31.28 \pm 2.35	73.68 \pm 0.14	10.06 \pm 4.67
Pre-Trained from ImageNet	25.65	79.14	4.07	28.14	79.05	18.66	26.90 \pm 1.76	79.10 \pm 0.06	11.37 \pm 10.32
Ours: IF-OM(ImageNet)	18.96	89.48	30.48	18.60	89.76	30.30	18.78 \pm 0.25	89.62 \pm 0.20	30.39 \pm 0.13

3 (see the main body). In this section, we will show the performance of each case under the cross-material and cross-dataset settings. Table A.3 presents the performance carried on LivDet2017 in the terms of Equal Error Rate (EER), Area Under Curve (AUC) and True Detection Rate (TDR) when False Detection Rate (FDR)=1.0%. Compared with the competing self-supervised methods, the proposed method achieves the best results among all the readers and metrics, which convincingly proves the effectiveness of IF-OM. The most significant improvement is carried on the case of Orcanthus, where IF-OM facilitates the baseline(ImageNet) from 71.46 % to 97.37 % in TDR@FDR=1.0%. When comes to the cross-dataset setting on face PAD, two cases, including [O,M] \rightarrow [C,I] and [C,I] \rightarrow [O,M] are considered. As listed in Table A.4, the similar improvement can be achieved by the proposed method. Typically, IF-OM can reach 73.58% AUC in the case of [C,I] \rightarrow [O,M], which significantly outperforms other solutions by a wide margin. Such results indicates the superiority of the proposed method over other self-supervised methods. The ROC curves with more detailed information is presented in Fig. A.2.

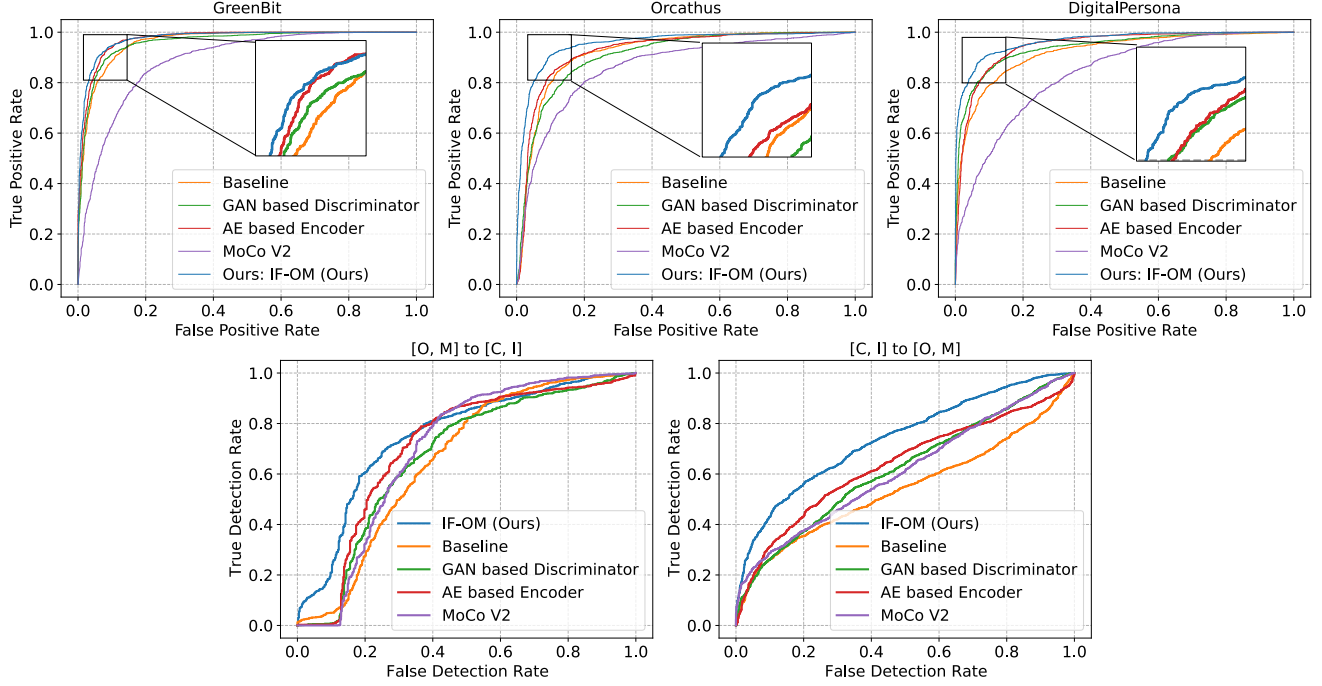


Figure A. 2. ROC curves for the proposed method and other self-supervised methods. The first row presents the cases on LivDet2017 under the cross-material setting. The second row refers to the face anti-spoofing under the cross-dataset setting on [O,M] and [C,I].

TABLE A. 5. Performance Comparison between the Proposed Method and the State-Of-The-Art Methods on LivDet2017 under the Cross-Material setting in the Terms of Average Class Error (%) \downarrow and TDR@FDR=1.0% \uparrow .

LivDet 2017	Single Model					Multiple Models (Ensemble Learning)			
	LivDet 2017 Winner	F.S.B		IF-OM(Ours)		FSB. + UMG Wrapper		RTK-PAD	
		ACE(%)	TDR(%)	ACE(%)	TDR(%)	ACE(%)	TDR(%)	ACE(%)	TDR(%)
GreenBit	3.56	3.32	91.07	2.78	94.14	2.58	92.29	1.92	96.82
Digital Persona	6.29	4.88	62.29	3.28	81.36	4.80	75.47	3.25	80.57
Orcanthus	4.41	5.49	66.59	1.38	97.37	4.99	74.45	1.67	96.18
Mean \pm s.d.	4.75 \pm 1.40	4.56 \pm 1.12	73.32 \pm 15.52	2.48 \pm 0.98	90.96 \pm 8.47	4.12 \pm 1.34	80.74 \pm 10.02	2.28 \pm 0.69	91.19 \pm 7.51

Comparison with the State-Of-The-Art Detector in Fingerprint

To further verify the effectiveness of the proposed method, we compare IF-OM with the state-of-the-art detectors on LivDet2017 under the cross-material and cross-sensor settings. As listed in Table A.5 and Table A.6, the proposed method has the great improvement compared with other single model based methods. A typical case is that, in the cross-sensor protocol, IF-OM can achieve 33.43% TDR@FDR=1.0%, while FSB only reaches 21.26%. Note that even compared with multiple model based methods, IF-OM also achieves very competitive results. In the terms of cross-material case, a 2.48% of ACE can be derived by our proposed method, which outperforms FSB+UMG Wrapper (4.12%) and is close to RTK-PAD (2.28%).

TABLE A. 6. Performance Comparison between the Proposed Method and the State-Of-The-Art Methods on LivDet2017 under the Cross-Sensor setting in the Terms of Average Class Error (%)↓ and TDR@FDR=1.0%↑.

Training (Testing) Readers	Single Model				Multiple Models (Ensemble Learning)			
	FSB		Ours:IF-OM		RTK-PAD		FSB+UMG	
	ACE(%)	TDR(%)	ACE(%)	TDR(%)	ACE(%)	TDR(%)	ACE(%)	TDR(%)
GreenBit (Orcanthus)	50.57	0.00	19.42	25.87	30.49	20.61	33.95	21.52
GreenBit (Digital Persona)	10.63	57.48	8.46	72.14	7.41	70.41	5.19	72.91
Orcanthus (GreenBit)	30.07	8.02	29.87	20.25	28.81	15.00	18.25	30.91
Orcanthus (Digital Persona)	42.01	4.97	27.21	7.94	29.19	13.26	23.64	28.46
Digital Persona (GreenBit)	10.46	57.06	7.49	53.03	6.74	70.25	3.65	85.21
Digital Persona (Orcanthus)	50.68	0.00	26.44	21.36	28.55	18.68	31.56	20.38
Mean \pm s.d.	32.40 \pm 16.92	21.26 \pm 28.06	19.82 \pm 9.80	33.43 \pm 24.12	21.87 \pm 10.48	34.70 \pm 25.30	19.37 \pm 12.88	43.23 \pm 28.31

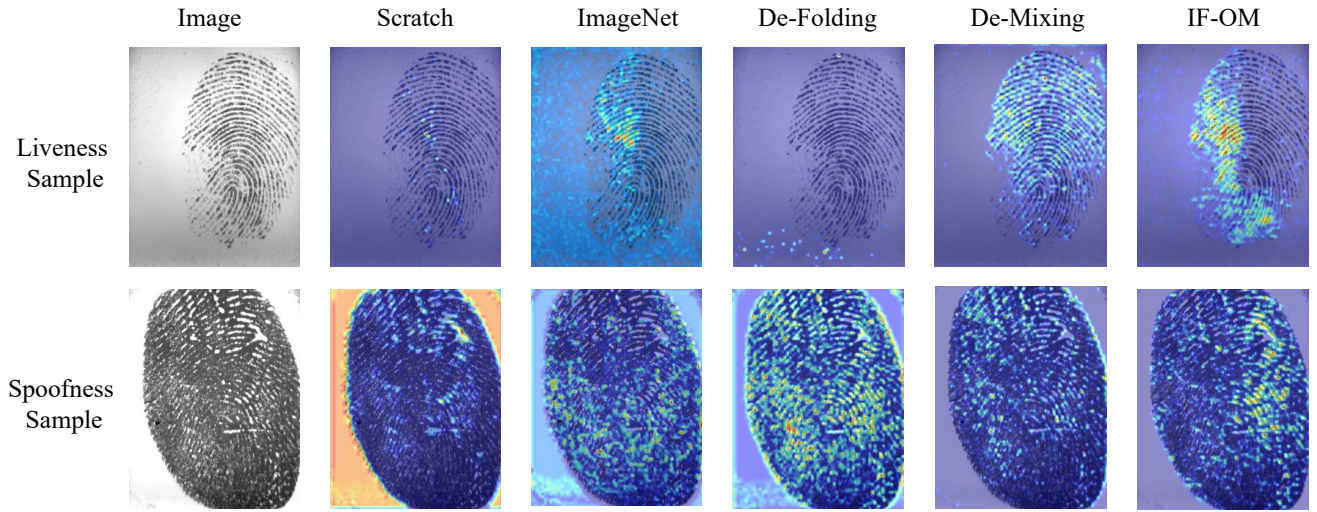


Figure A. 3. The Grad-CAM based visualization on LivDet2017 using Digital Persona. The first row shows the liveness sample and the second row presents the spoofness sample. Note that the visualized model is not trained by PAD task.

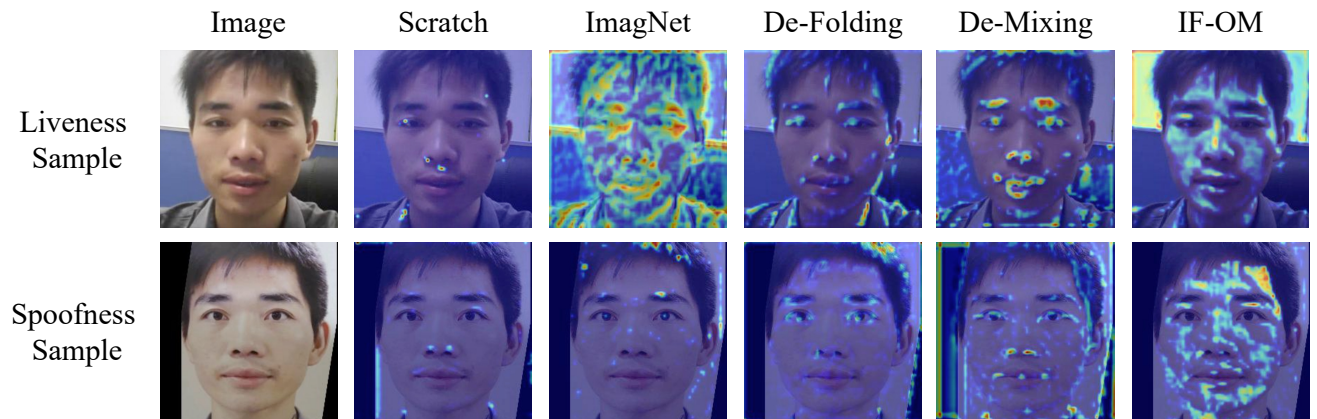


Figure A. 4. The Grad-CAM based visualization on CASIA-FASD. The first row shows the liveness sample and the second row presents the spoofness sample. Note that the visualized model is not trained by PAD task.

Visualization Results

To further investigate the advance of the proposed method over other baselines, we visualize the discriminative features extracted by the models with same architecture but different initialization. As shown in Fig. A.3, IF-OM can localize the adequate discriminative features for both liveness and spoofness samples. However, in the terms of De-Folding and De-Mixing, only partial features can be extracted. When compared with the pretrained model from ImageNet, IF-OM does not localize any background information as the initialized features, which indicates the effectiveness of the proposed method. When comes to the face PAD, similar performance can be observed in Fig. A.4. Typically, for the given spoofness sample, only IF-OM can localize the effective region for PAD.